NTNU
Norwegian University of
Science and Technology

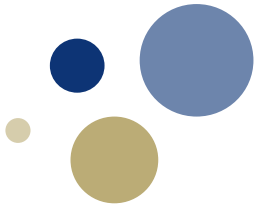

Barents Sea Ice Edge Position Variability 1579-2018

Harald Yndestad,

NTNU Ålesund

Last Update: 12.09.2019

http://www.ntnu.no/ansatte/harald.yndestad
NTNU in Ålesund, Postboks 1517, NO-6025 Ålesund, Norway
http://www.ntnu.edu/alesund

1 INTRODUCTION

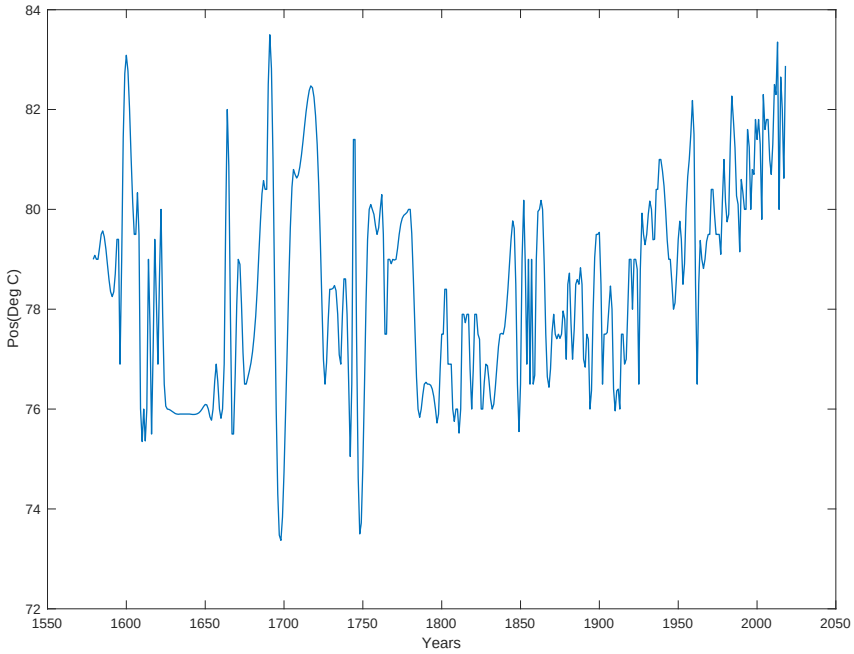

Figure 1. The Barents Sea Ice edge position 1800-2016.

Figure 1 show the Barents Sea ice edge position data series from 1579-2018, which cover a period of 439 years. The data series analysis is split in two parts. The best part covers a 218-year periods from 1800 to 2018. In this time period the data series has 153 recorded data points and 66 cubic spline interpolated data points. In this time period we can estimate stationary periods up to 218/2 = 109 years. From 1579 to 1800 the data series has 83 recorded data points and 139 data points interpolated by cubic spline interpolations, shown as continues lines on Figure 1. The total data series cover a period of 439 years which may represent reliable periods up to 220 years. In this long data series, missing data is expected to be estimated in the power spectrum.

The research questions

The research questions in this investigation are:

- To identify possible deterministic periods in Barents Sea ice edge position data series.
- To compute upcoming events
- To identify the influence on the NAO winter index

Climate periods and marine biomass periods

The British astronomer Edmond Halley (1656-1742) was probably the first to publish a paper on climate influence on biomasses in the North Sea. Halley tried to solve the problem of the determination of longitude and conducted pioneering investigations in geophysics, trade winds, tides, the magnetism of the earth and the relationship between the weather and dynamic air pressure. He estimated the longitude by observing the 18.03-year lunar saros cycle, the cycle that is associated with the time between eclipses. Using this approach, he published a method that he claimed to be accurate within 69 miles at the equator. In 1699 he sailed in the Atlantic and made magnetic maps. In the paper *Atlas matitimus et commercialis* of 1728 he described the theory of a fluctuating herring stock between the Arctic Ocean and the North Sea, controlled by climate conditions (Wegner, 1993).

The Ljungman solar-theory

The solar theory goes back to Ljungman (1879, 1882). The Swede Axel Ljungman studied records from Bohuslan herring fisheries from 1000 A.D. and found herring periods of 30 to 60 years. Ljungman

presented the theory that long-term biomass fluctuation of herring was related to a 111-year sunspot cycle (Ljungman, 1879). In 1960´s R. G Currie started to analyze a number data series by Maximum Entropy spectrum analysis. He identified the 11-year solar cycle in the Earth rotation, the temperature in North America and world weather records (Currie et al. 1987). Later the 11-year solar period has been identified in a number of other investigations of global climate indicators. The solar-Arctic ice theory is based on the idea that there is a positive feedback between radiation from the Sun and melting of Arctic ice. Melting of Arctic ice leads to less reflection of sunlight from Arctic ice and more warming of Arctic seawater. Arctic ice extent variability then will be amplified.

The Pettersson lunar-wave theory

In 1909, the Swedish oceanographer Dr. Otto Pettersson (1848-1941) studied the relationship between herring catches and tides in Gullmarfjord on the west coast of Sweden. The study showed that the variation in the lunar perigee was related to freshwater movements and the arrival of schools of herring. As the ocean water presses in toward that inland sea, it dips down, allowing fresh surface water to roll out above it. At that depth, where salt and fresh water come into contact, a sharp layer of discontinuity forms, much like the surface film between water and air. This salt layer has a vertical fluctuation in long time series. Pettersson found that the fluctuation correlated with the moon's phases, long-period tides and long-period herring catches. Pettersson argued that there were two types of tides; the *diurnal and the semi-diurnal tide* caused by the rotation of the earth under the gravitational field of the sun and the moon, and *the parallactic tide*. This tide depends upon the varying distance of the sun and the moon and their position with respect to the earth. By analyzing these distances, he found oscillating periods of 9, 18, 93, 111, 222 and up to 1433 and 1850 years. The most important cycle was the 18.09-year saros cycle and the 111-year cycle that he called "The Greater Saros" (Pettersson; 1914b, 1915, 1930; Hans Pettersson, 1915). In 1887, the German geography professor Otto Krümmel (1854-1912) published the first major handbook on modern oceanography. Here, Krümmel had a critical commentary on the importance of long tidal waves, discovered by Georg H Darwin (son of Charles). At a time when modern science was being created, the Moon was not a politically correct explanation, and wind-theory from Zöppritz and the comment from Otto Krümmel were widely accepted up to our time.

Russian scientists. Izhevskii (1961, 1964) and other Russian scientists developed a system view of the Atlantic Ocean, Arctic and the Barents Sea. Maksimov and Smirnov (1965, 1967) identified a standing 18.6-year lunar nodal tide as a standing wave in Atlantic Oceans. Malkov (1991, 2002) identified a statistical relationship between earth pole movements and biomass fluctuations in the Barents Sea. Ottestad (1942) investigated landings in Lofoten from 1875 to 1940. Cycles were identified by a visual inspection of similarities in fluctuations. He found maximum cycles of Northeast Arctic cod at intervals of 11, 17.5, 23 and 57 years. The cycles were compared to fluctuations in tree rings from Troms and the conclusion was that biomass fluctuations must be influenced by climate fluctuations. Later he compared sunspot cycles and biomass cycles (Ottestad, 1979). Wyatt et al. (1994) investigated the time series of cod landings records from Lofoten and found a cycle of 18.6 years. The cycle was explained by the influence from the 18.6-year lunar tide. Yndestad introduced new wavelet spectrum analysis methods and identified a lunar spectrum [18.6/3, 18.6, 3*18.5, 4*18.6] (yr.) in data series of sea-level from Aberdeen, Oslo-fjord to Murmansk, temperature and salinity in inflow of North-Atlantic water to the Norwegian Sea and the Barents Sea, sea temperatures and rainfall in Norway, Arctic Ice extent in the Barents Sea, Earth axis movements and the marine eco-system in the Barents Sea (Yndestad 1999a, 1999b, 2004, 2006, 2009), (Yndestad et al. 2008). The lunar nodal spectrum is explained by a chain of events between the Atlantic Ocean and the Arctic Ocean. Egbert and Ray (2000) show that about 1 TW, or 25–30% of the total dissipation, occurs in the deep ocean. The estimated mixing energy required to maintain the large-scale thermohaline circulation is about 2TW. One-half could therefore be provided by the tides.

The Zöppritz wind-theory

The German mathematician Karl Zöppritz (1838-1885) developed a model that showed over time the wind can affect water at great depths. Helland-Hansen and Nansen (1909) found a relationship between the air temperature at the Ona light and fluctuations of Northeast Arctic cod. Helland-Hansen and Nansen concluded that there is a climatic influence on biomass fluctuations. After Nansen, the wind-theory has been widely accepted. This theory has characterized the view of the changes in Arctic climate right up to our time and support the foundation the understanding global warming and Arctic ice position variability, as a process, driven by greenhouse gasses.

The NAO index represents is a wind-theory indicator. The North Atlantic Oscillation (NAO) is a weather phenomenon in the North Atlantic Ocean of fluctuations in the difference of atmospheric pressure at sea level between the Icelandic low and the Azores high. Through fluctuations in the strength of the Icelandic low and the Azores high, it controls the strength and direction of westerly winds and location of storm tracks across the North Atlantic. Positive values of the NAO index are associated with low atmospheric pressure difference between Iceland and Azores. In Scandinavia it causes warm winds from west, mild winters and rain-full summers. Negative values of the NAO index are associated with high atmospheric pressure difference between Iceland and Azores. In Scandinavia it causes cold winds from north, cold winters and less rain-full summers. The NAO winter index variability has a period coincidence to lunar periods in North Atlantic Water variability and Arctic ice extent (Yndestad et al. 2008; Yndestad 2006). Dickson et. al, 2000 confirmed a correlation between the NAO winter index and Arctic Ocean water inflow temperature (50-500m) and a correlation between NAO winter index and Fram Strait Ice flux (km2/yr.). The study concludes "direct regional wind forcing over broadscale changes in the Arctic Ocean circulation in determining the year-to- year variability of ice flux". Yndestad (2006) and Yndestad et. al (2006) studied the wavelet specter of North Atlantic Water temperature, the Barents Sea (Kola) data series, Arctic air temperature, Barents Sea ice extent, Greenland Sea ice extent and the NAO winter index. The result show that Barents Sea ice extent is controlled by lunar period in North Atlantic Water and the NAO index is controlled by the mean Greenland and Barents Sea ice extent. Smedsrud, L. H., et al. (2013) studied the wind-feedback hypothesis between air heat transport and Atlantic heat transport and the ocean-feedback hypothesis. The study concluded: "The Barents Sea marine climate is set by the ocean and the presence of warm Atlantic Water, but the atmosphere governs variability on time scales shorter than a year. If the sea ice disappears, the atmosphere may be more dominant in the future."

This study

This study is based on wavelet spectrum analysis to identify stationary periods and period phase-relations in the Barents Sea ice edge (BIE) position, Barents Sea temperature and the NAO winter index. BIE is controlled by Barents Sea temperature variability if, and only if, the periods have the same periods- and phase-relations. The NAO index is controlled by BIE if, and only if, the NAO index has the same periods- and phase-relations.

2 MATERIALS AND METHODS

2.1 Materials

Barents Sea ice edge position

The Barents Sea ice edge position data series covers the position in August between Svalbard and Franz Josef Land for the period 1579-2018, given as the mean latitude within the sector 20 –45°E. The data series is updated from Vinje (1999) *(Falk-Petersen et al. 2015)* (personal communication) and contains 236 annual values from a time period of 439 years. The 203 gaps in the data series is cubic spline interpolated (MATLAB) by Harald Yndestad.

Kola section temperature data series

The Kola section temperature data series is provided by the Polar Research Institute of Marine Fisheries and Oceanography (PINRO), Murmansk in Russia (Vladimir Ozhigin, personal communication). The data used here are monthly temperature values from the upper 200 m of the Kola section along the 33°30'E medial from 70°30'N to 72°30'N in the Barents Sea (Bochkov, 1982; Tereshchenko, 1997). The temperature data series contains quarterly and annual values from the period 1900 to 2005 and monthly values from 1921 to 2005, some of which are measured and some of which are calculated. The gaps in the time-series were filled by Bochkov (1982) by means of calculations by multiple regression models. This presentation covers the annual mean temperature from 1900-2017.

North Atlantic Oscillation

The North Atlantic Oscillation (NAO) is defined as the normalized pressure difference between a station on the Azores and one on Iceland. The NAO index analysis is based on the official data from Climate Research Unit and covers the years 1822 until 2018. The data series is obtained from the Internet address

http://www.cru.uea.ac.uk/cru/data/nao.htm. In this presentation the NAO winter index is computed as the annual mean temperature from December to March.

2.2 Methods

The stationary solar-lunar periods in the temperature data series are identified in the wavelet spectra. The stationary period time and period phase are estimated by computing the wavelet autocorrelations, the wavelet power spectrum and the wavelet phase spectrum. A wavelet transform separates a data series x(t) based on a moving correlation into a set of scaled data series. To reduce false periods, all data series are scaled prior to the wavelet analysis by the following:

$$x(t) = y(t) - E[y(t)])/var[y(t)] \quad (1)$$

where y(t) is the data series, E[y(t)] is the mean value, var[y(t)] is the variance and x(t) is the scaled data series. The scaled data series are transformed into a wavelet spectrum by the following:

$$W_{a,b}(t) = \frac{1}{\sqrt{a}} \int_R x(t)\, \Psi\left(\frac{t-b}{a}\right) dt \quad (2)$$

where $x(t)$ is the analyzed time series; Ψ() is a coif3 wavelet impulse function [63], [64], which is chosen for its symmetrical performance and its ability to identify symmetrical periods in data series; $Wa,b(t)$ represents the computed wavelet spectrum; parameter a represents a time-scaling parameter; and parameter b represents a translation in time for the wavelet transformation. When translating $b = 0$ and s = 1/a, the wavelet spectrum W(s, t) represents a set of moving correlations between $x(t)$ and the impulse function Ψ() over the entire time series $x(t)$. The relationship between wavelet s and sinus period T is approximately $T \approx 1.2$ s when using the coif3 wavelet function. In this investigation, the transformed wavelet spectrum W(s, t) has a set of wavelet functions in the spectrum range s = 0, 1, 2…0.6N, where N is the number of samples in the data series. W(s(min, -0, max, +0), F) represents a wavelet s that has a. dominant phase state W(s(max), F) = [min, -0, max, or +0], at a year t = F. The wavelet power spectrum is computed by the following transform:

$$WP(s, t) = W(s, t)*W(s, t) \quad (3)$$

The wavelet power spectrum identifies the most dominant wavelets in the wavelet spectrum W(s, t). WP(s(max) F) = [s(min, -0, max, +0), F] represents a wavelet power spectrum where the maximum amplitude has phase-shifts [min, -0, max, +0] at the time vector F (yr.). A wavelet spectrum W(s, t) is transformed into a set of autocorrelations by the following transform:

$$WA(R(s), m) = E[W(s, t)W(s, t + m)] \quad (4)$$

where WA(R(max), T) = (R, T) represents a wavelet s that has a correlation R to a stationary period T. A stationary period T in WA(R(s), m) has a set of subharmonic periods at m = [T, 2T, 3T…] (yr.). A set of autocorrelations may have coincidence periods of WA(R(max), m) = [(R1, k*T1), (R2, p*T2)] for k*T1 = p*T2.

2.3 Theory

This investigation is based on the simple idea that we may compute upcoming event in Barents Sea ice edge variability if, and only if, we are able to identify stationary periods in the data series. Possible stationary periods are lunar periods and solar periods. Stationary periods in the data series are identified by wavelet spectrum analysis.

Solar-Lunar periods

Stationary lunar periods are associated with the relation between the Earth, the Moon and the Sun. In this investigation the lunar periods are based on the first periods: [Tln(perigean), Tln(nodal)] = [8.8475, 18.6134]. The first periods may have a lunar period harmonic spectrum: Tln() = [K1*8.8475, K2*18.6134], for (K1, K2) = 1,2,3… The 18.61-year lunar nodal period is related to the 18.61-year Earth axis nutation and the 18.61-year lunar nodal tide. The 18.61-year Earth nutation

standstill period has the period and phase: Sln(Tln, Fln(still)) = (18.61, 1951.19) (yr.). From the lunar nodal standstill, there is a $\pi/2$ (rad) phase-lag to the standing 18.61-year lunar nodal tide between Earth's equator and poles, which is approximately at a maximum at Sln(Tln, Fln(max tide)) = (18.61, 1983.77) (yr.). From the lunar nodal tide, there is a $\pi/2$ (rad) phase-lag to an 18.61-year lunar nodal ocean temperature oscillation, which has a maximum at approximately Sln(Tln, Fln(max temp)) = (18.61, 1941.49) (yr.). A wavelet spectrum analysis of North Atlantic water entering the Norwegian Sea estimated an 18.61-year lunar tide maximum in 1950 and an 18.6-year lunar temperature period maximum in 1942 (Yndestad et al. 2008).

Solar periods are associated with the periods from the large planets Jupiter, Saturn, Uranus and Neptune: Ttsi() = [(Tvel(22.14), Tju(11.862), Tsa(29.447), Tur(84.02), Tne(164.79)] (yr). The first solar planets may have an harmonic spectrum Ttsi() = [(P1*Tvel(22.14), P2*Tju(11.862), P3*Tsa(29.447), P4*Tur(84.02), P5*Tne(164.79)] (yr), for (P1, P2, P3, P4, P5) = 1, 2, 3….. TSI-HS data series from 1700-2014, has identified the stationary solar periods: Ttsi = [11, 84, 164, 5*84/2=210, 9*84/2=373] (yr.) (Yndestad and Solheim, 2017). Solar-lunar period coincidences are expected to influence global temperature oscillations. Solar and lunar periods have coincidences of: [2Tsa(29.45), 7Tln(8.847)] = [58.90, 61.13], [6Tsa(29.45), 20Tln(8.847)] = [176.7, 176.9], [15Tsa(29.45), 5Tur(82.04), 24Tln(18.61)] = [411.98, 420.1, 446.72]

Period identification

Stationary periods in Barents Sea ice edge position variability (Wie(s(t)) are identified by computing the period- and phase difference:

$$E(Ae, Te, Fe) = [S(As, Ts, Fs) - Wi(Ti, Fi)] \quad (5)$$

where S(As, Ts, Fs) represents a stationary period that has an amplitude vector As, a period vector Ts and phase-vector Fs. W(A, T, F) represents an identified wavelet spectrum that has an amplitude-vector Ai, a period-vector Ti and a phase-vector Fi.

3 RESULTS

3.1 Arctic ice edge position variability

3.1.1 Ice edge position variability 1800-2018

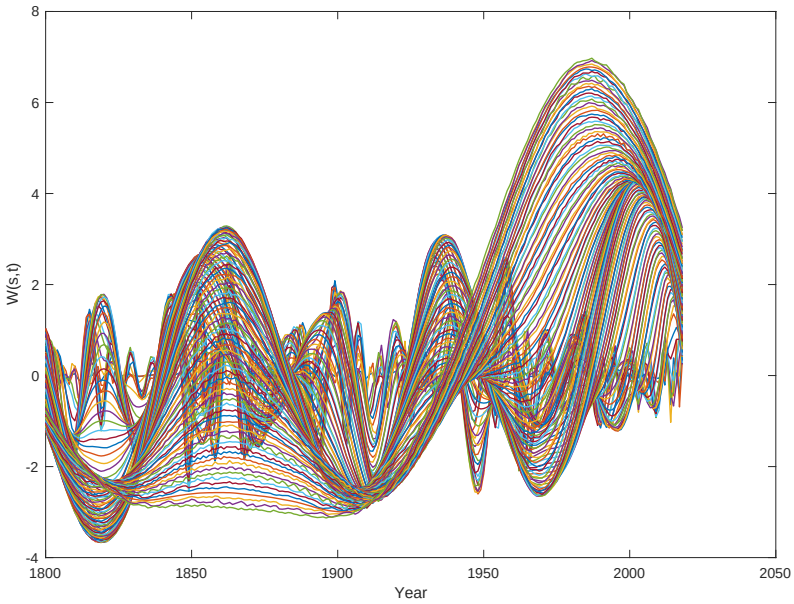

Figure 2. The Barents Sea ice edge position wavelet autocorrelation spectrum Wie(s, t) for s = 1...130 and t = 1800...2018.

The Barents Sea Ice edge position data series (Figure 1) is transformed into a wavelet spectrum Wei(s, t) for s = 1…130 and t = 1800…2018 [Eq. 2] (Figure 2). The dominant period in the wavelet spectrum has amplitude and phase-shifts at: Wie(s(max), Fie) = [(+0,1800), (-3.4, 1818), (-0, 1838), (3.2, 1859), (+0, 1882), (-2.8, 1906), (-0, 1925), (2.9, 1943), (+0, 1962), (-2.5, 1970), (-0, 1992), (4.3, 2010)]. The wavelet spectrum phase-shifts have mean distances of [18, 20, 21, 23, 24, 19, 19, 19, 15, 15, 15] (yr), or a mean distance of 18.8 years. The total period is 4*18.8 = 75.2 years. The coincidence between the identified long BIE period and the deterministic lunar nodal period is: [Tie(75.2) – Tln(4*18.6)] = 0.7 years. The wavelet spectrum confirms that Arctic ice position variability from 1800 AD, has a stationary lunar period of 4*18.6 = 74.4 years.

The stationary period has the computed upcoming phase-shifts of: Wie(s(max/0), Fie) = [(+0, 2029), (min, 2047), (-0, 2066), (max, 2085)]. More ice extent to a minimum position and colder period from 2029 to a deep minimum close to 2047 A.D. From 2047 the position increases to a maximum close to the year 2085.

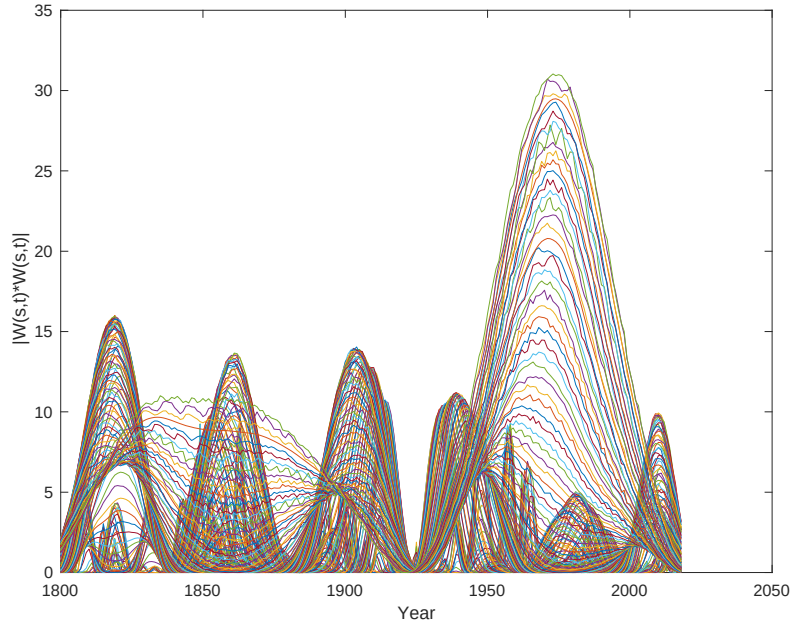

Figure 3. The Barents Sea Ice edge position Wavelet Power Spectrum 1800-2016 for t = 1800…2018 and s = 1…130.

The Barents Sea ice edge position wavelet spectrum Wie(s, t) is transformed into a wavelet power spectrum WPie(s, t) as shown on Figure 3. The computed Barents Sea ice position wavelet power spectrum from 1800 to 2018 has a maximum and phase-shifts at the years: WPie(s(max), Fie) = [(16.5, 1819), (-0, 1840), (14.8, 1861), (+0, 1888), (-15.8, 1903), (-0, 1924), (13.2, 1937), (+0, 1964), (5.9, 1981), (-0, 1994), (19.7, 2010)]. The wavelet power spectrum maximum has a mean time distance of 37 years and confirm mean total wavelet period of 2*37=74 years.

The wavelet power spectrum has the same period amplitude, which confirm a stationary 74.4-year climate period. At the same time Figure 5 show a longer period that has a maximum (cold climate) close to 1850 and a maximum (warm climate) close to 1975. This period explains why there was the long ice position trend from a warmer climate, from 1850 to 2018 (Figure 2). The Barents Sea ice edge position variability has longer periods.

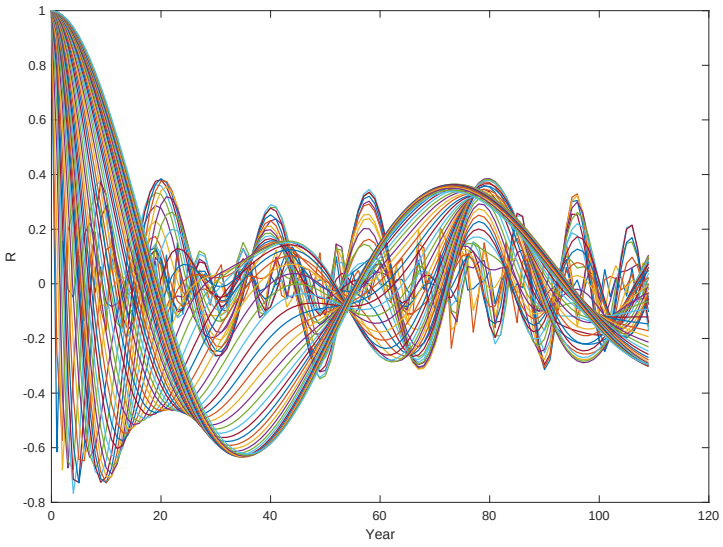

Figure 4. The Barents Sea ice edge position wavelet autocorrelation spectrum WAie(R(s), t) for s = 1…130 and t = 1800…2016.

Stationary periods in Wei(s, t) are identified by computing the autocorrelations WAie(R(s), m) [Eq. 4] as shown on Figure 4. The computed autocorrelations in the wavelet specter has the correlations to the dominant periods: WAie(R, T) = [(0.40, 9), (0.40, 19), (0.30, 40), (0.35, 57), (0.52, 74)], which show a correlation vector R = [0.40, 0.44, 0.40, 0.30, 0.52] to the stationary periods Tie = [9, 19, 40, 57, 73] (yr.). The coincidence difference to the 18.6-year lunar nodal period spectrum Tln = [18.6/2, 18.6, 2*18.6, 3*18.6, 4*18.6] is [Tie – Tln] = [0, 1, 3, 1, 1] (yr.), which has a mean difference of 1 year. The autocorrelation wavelet specter represents a data series "fingerprint". The close coincidence to the lunar spectrum represents an evidence of a lunar-driven control of Barents Sea ice edge position variability.

3.1.2 Ice edge position variability 1579-2018

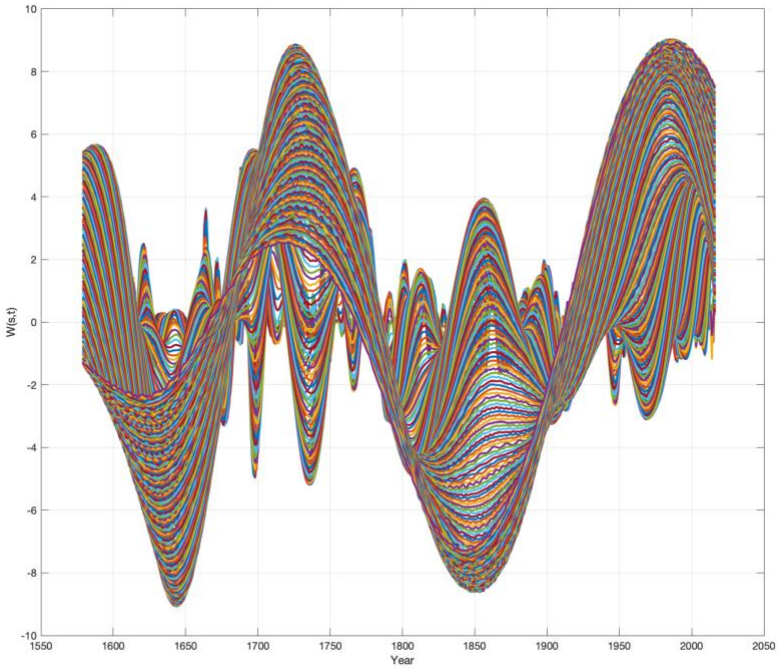

Figure 5. The Barents Sea ice position Wie(s, t) wavelet spectrum for s = 1…250 and t = 1579…2018.

The Barents Sea ice edge position data series (Figure 1) is transformed into a wavelet spectrum Wei(s, t) for s = 1…250 and t = 1549…2018 [Eq. 2] (Figure 5). The dominant periods in the wavelet spectrum has amplitude and phase-shifts at: Wie(s(max/0), Fie) = [(-8.9, 1643), (-0, 1680), (8.7, 1725), (+0, 1783), (-7.2, 1849), (-0, 1911), (9.0, 1986)]. The wavelet spectrum has phase-shifts in a mean distance of 57.2 years and a total mean period of 4*57.2 = 228.8 years. The period distance between the identified periods and the stationary lunar periods are: [(57.2 – 3*18.6), (228.8 – 3*4*18.6)] = [1.4, 5.5] years. The identified 223-year lunar period has phase-shifts of: Wie(s(max/0), Fie) = [(+0, 1582), (-6.2, 1634), (-0, 1681), (7.7, 1732), (+0, 1786), (-7.7, 1850), (-0, 1919), (8.5, 1986)].

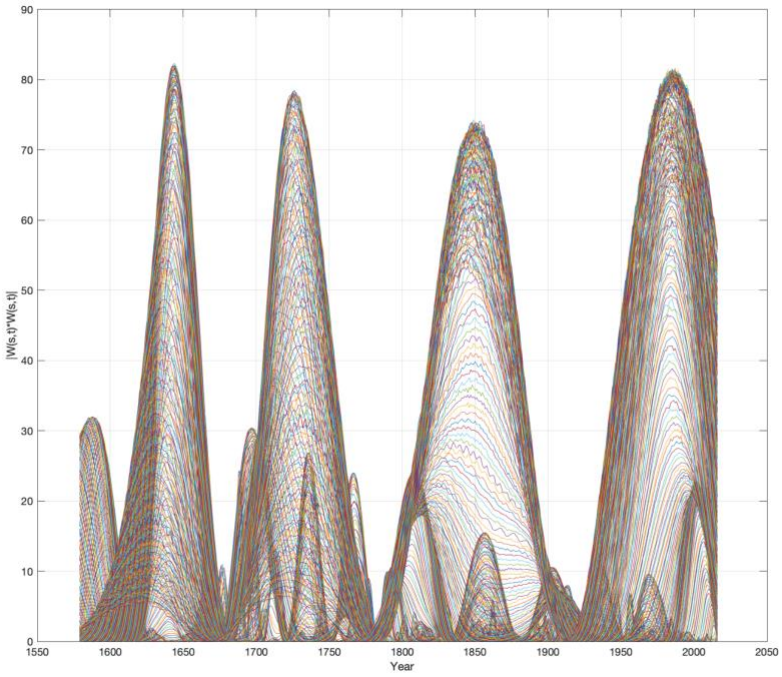

Figure 6. Wavelet power spectrum WPie(s, t) of the Barents Sea ice extent wavelet spectrum for t = 1579…2018 and s = 1…250.

Figure 6 shows the wavelet power spectrum of the Barents Sea ice position for t = 1579…2018 and s = 1…250. The dominant periods in the wavelet power spectrum has a maximum and phase-shifts at: WPie(s(max), Fie) = [(+0, 1580), (-82.0, 1649), (-0, 1680), (+78.0, 1726), (+0, 170), (-73.9, 1850), (-0, 1920), (+81.6, 1987)]. The mean periods phase-shift distance is 58 years. The total period is 4*58 = 232 years. The estimated coincidence to the lunar period is: (232 – 3*4*18.6) = 8.6 years, which is close to the 4*74.4 = 223.2 year lunar period. The wavelet power spectrum on Figure 6 confirm the close relation between the identified 74-year and 223-year lunar-driven periods in Arctic ice position variability. Wavelet power periods of 223/2 = 111.6 year are related to harmonic periods of 3*74.4/2 = 111.6 years.

Upcoming events

The stationary 223-year lunar-driven power period has the computed upcoming phase-shifts: WPie(s(223), Fie) = [(+0, 1850 + 3*223/4 = 2018), (min, 1850 + 223 = 2073), (-0, 2018 + 223/2 = 2130), (max, 2073 + 223/2 = 2185)]. The period has computed phase-shift close to the year 2018, a deep minimum position, maximum ice extent and maximum cold climate close to the year 2073 A.D. The stationary 74-year lunar-driven period has the computed upcoming phase-shifts of: Wie(s(max/0), Fie) = [(+0, 2029), (min, 2047), (-0, 2066), (max, 2085)]. The 74-year period and the 223-year period is negative at the same time in the period 2029 to 2066 A.D. We may then expect a computed minimum ice position and a deep Arctic temperature minimum close to 2070 A.D.

3.2 Barents Sea temperature variability

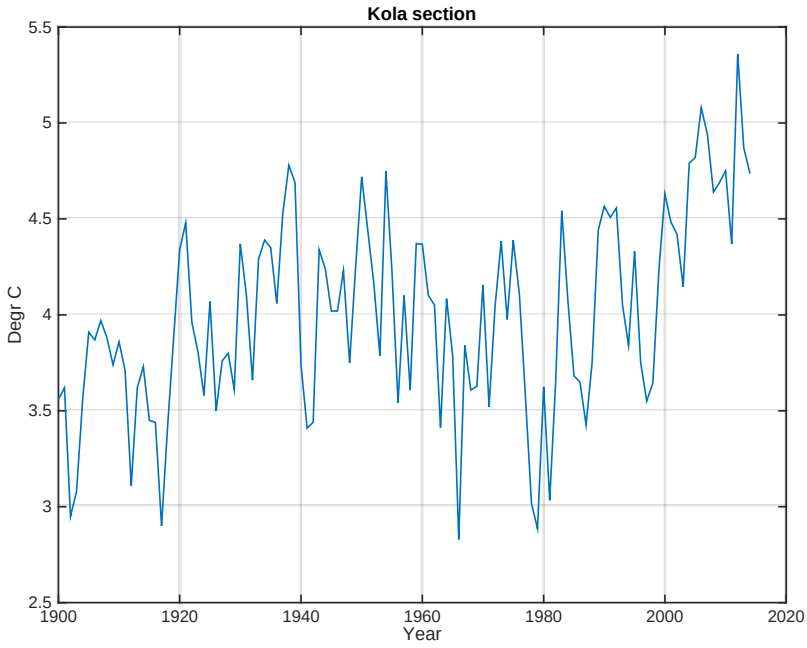

Figure 7. The Barents Sea Kola section data series from 1900 to 2015.

North Atlantic Water controls the climate of the northern part of Europe. The water current passes the Faroe-Shetland Channel and into the Norwegian Sea and continues north with a minor inflow to the Barents Sea. In the Barents Sea Kola section, the water temperature has been monitored since 1900 and the Kola-section data series (Figure 7) represents the longest oceanographic temperature data series in the world. The data series represents an indicator of Arctic climate and expected Barents Sea biomass growth. The Barents Sea temperature has grown the last 30 years to a level, far above historical records.

The computes wavelet spectrum Wko(s, t) for s = 1...60 and t = 1900...2115 has dominant wavelet and amplitude and phase-shift at: Wko(s(max), Fko) = [(-3.1, 1911), (-0, 1920), (3.8, 1943), (+0, 1960) (-4.8, 1978), (-0, 1993), (4.8, 2006)]. The mean time between phase-shifts is 19 years in a total period of 76 year. The coincidence to the lunar periods is [0, 2] (yr). The wavelet autocorrelations have a maximum at: WAko(Rko(max), Tko) = [(0.2, 9), R(0.5, 18), R(0.32, 36, 76)].

Period coincidence
The coincidence difference from lunar period is: [Tko - Tln] = [(9, 19, 34) - (18.6/2, 18.6, 2*18.6, 4*18.6)] = [0, 0, 0, 2] (yr.), or a mean difference of less than 1 year.

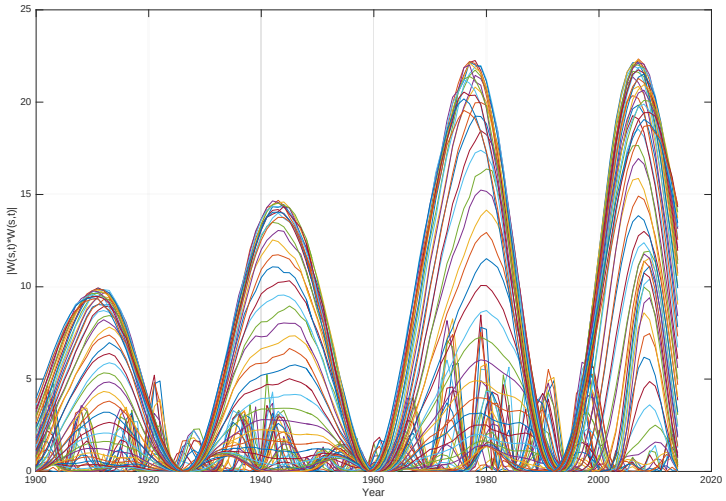

Figure 8. Wavelet power spectrum WPko(s, t) of the Barents Sea Kola wavelet spectrum Wko(s, t), for s=1...60 and t =1…2015.

Wavelet power spectrum WPko(s, t) of the Barents Sea Kola wavelet spectrum Wko(s, t), for s = 1...60 and t = 1…2015, is shown on Figure 8. The wavelet power spectrum WPko(s, t) has a maximum and phase shifts at: WPko(s(max), Fko) = [(10.0, 1911), (-0, 1926), (14.5,1943), (+0, 1959), (22, 1978), (-0, 1994), (23, 2007)]. The mean distance between the period phase-shifts is 17 years, which confirm a 18,6-year lunar period coincidence.

Barents seas ice position coincidence

The Barents Sea ice edge position variability has the stationary periods: Tie = [9, 18, 34] (yr). The period coincidence difference to Barents Sea ice position periods are: [Tko – Tie] = [(9, 18, 36) – (9, 20, 34)] = [0, 1, 2] (yr.), or a mean period difference of 1 year. The stationary periods in Barents Sea ice edge position have phase-shifts of: Wie(s(max/min), Fie) = [(+0, 1800), (-4.0, 1818), (-0, 1838), (3.7, 1859), (+0, 1882), (-3.8, 1906), (-0, 1925), (3.4, 1943), (+0, 1962), (-2.0, 1977), (-0, 1992), (2.3, 2007)]. The phase-shift coincidence difference from the Barents Sea temperature shifts are: [Wko(s(max/min), Fko) - Wie(s(max/min), Fie)] = [5, 1, 0, 3, 1, 2, 0] (yr), or a mean phase-difference of only 1.7 years. This close relation shows that Barents Sea ice edge position variability is periods- and phase-locked to the Barents Sea Kola-section temperature variability.

Upcoming events

The stationary 74-year period in the wavelet specter Wko(s(74), t) has the computed upcoming events: Wko(s(max), Fko) = [(14.5,1943), (+0, 1959), (-22, 1978), (-0, 1994), [(max, 2007), (+0, 1959 + 74 = 2033), (min, 1978 + 74 = 2052), (-0, 1994 + 74 = 2068), (max, 2007+74 = 2081)]. The close relation between Barents Sea ice edge position and Barents Sea Kola section temperature confirm a possible 223-year Barents Sea temperature period that have the phase-relations close to: Wko(s(223), Fie) = [(+0, 2025), (min, 2080), (-0, 2143), (max, 2196)]. The computed upcoming periods reveal a and upcoming cold Barents Sea temperature period from 2025 to 2143.

NAO Index variability coincidences

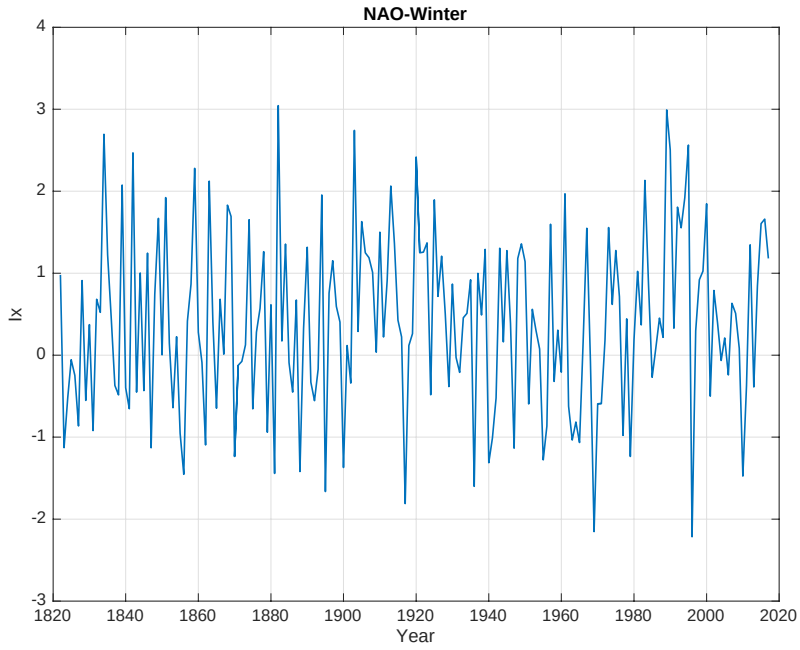

Figure 9. The NAO-winter index data series from 1822 to 2017.

The North Atlantic Oscillation (NAO) is a weather phenomenon in the North Atlantic Ocean of fluctuations in the difference of atmospheric pressure at sea level between the Icelandic low and the Azores high. Through fluctuations in the strength of the Icelandic low and the Azores high, it controls the strength and direction of westerly winds and location of storm tracks across the North Atlantic. The NAO winter index is based on the (December thru March) station-based difference of the normalized sea level pressure. Positive values of the NAO index are associated with low atmospheric pressure difference between Iceland and Azores. In Scandinavia it causes warm winds from west, mild winters and rain-full summers. Negative values of the NAO index are associated with high atmospheric pressure difference between Iceland and Azores. In Scandinavia it causes cold winds from north, cold winters and less rain-full summers. Figure 10 shows the annual NAO winter index from 1822 to 2017. The NAO winter index is computed by (December (n-1)+January (n)+February (n) + Mars (n))/4.

The identified 74-year period in the wavelet spectrum Wnao(s, t) has amplitude and phase-shifts at: Wnao(s(74), Fnao) = [(-0, 1832), (0.4, 1852), (+0, 1862), (-1.2, 1888), (-0, 1899), (2.2, 1919), (+0, 1937), (-2.9, 1957), (-0, 1977), (2.3, 1990), (+0, 2017)]. In the same time period the identified stationary 74-year period has amplitude and phase-shifts at: Wie(s(74), Fie) = [(+0, 1800), (-4.0, 1818), (-0, 1838), (3.7, 1859), (+0, 1882), (-3.8, 1906), (-0, 1925), (3.4, 1943), (+0, 1962), (-2.0, 1977), (-0, 1992), (2.3, 2007)]. The phase-coincidence between the NAO index and the and Barents Sea ice edge position is: [Wie(s(74, +0), Fie = 1943) - Wnao(s(74, +0), Fie = 1937)] = 6 years. This mean there is close to a (π/2) (rad) phase-lag between NAO variability and Barents Sea ice edge position variability.

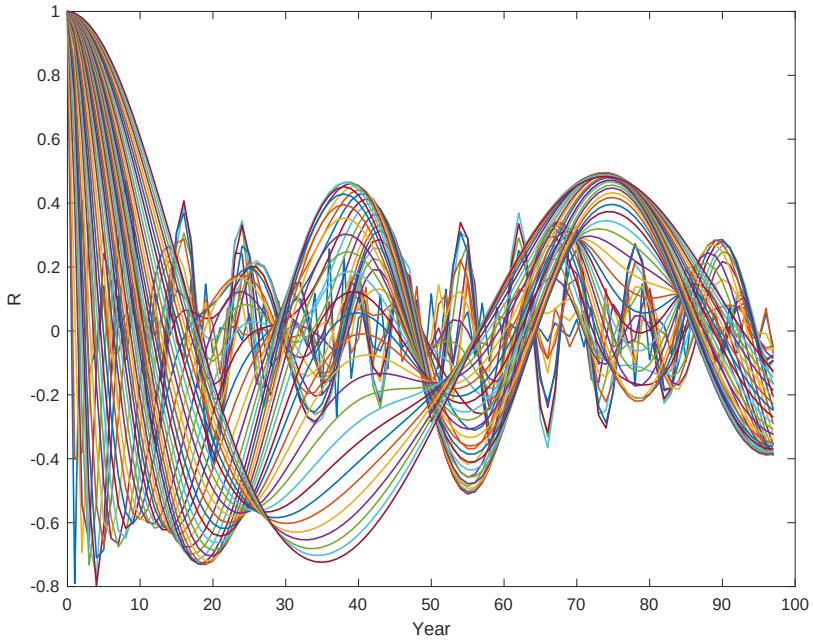

Figure 10. Autocorrelation spectrum WRnao(R(s), m) of the Kola wavelet spectrum W(nao, s, t) for s=1 to 0.6N and m=0 to 58.

Figure 10 shows the computed wavelet autocorrelations WRnao(R(s), m) of the NAO Index wavelet spectrum W(nao, s, t). The wavelet autocorrelation wavelet spectrum identifies a correlation to the stationary periods: WRnao(Rnao, Tnao) = [(0.48, 8), (0.40, 16) (0.47, 38), (0.5, 74)], which represents a correlation Rnao = [0.48, 0.40, 0.47, 0.5] to the periods Tnao = [8, 16, 38, 74] (yr). The coincidence difference to lunar periods is: [Tnao - Tln] = [(8, 16, 38, 74)-(8.85, 18.6, 2*18.6, 4*18.6)] = [0, 2, 3, 0], or a mean distance of 0.8 years.

Ice edge position coincidence

The 74-year stationary periods in Barents Sea ice extent and NAO index has a phase-coincidence [Fie(74) – Fnao(74, -π/2)] = [(1838, 1859, 1882, 1906, 1925, 1943, 1962, 1977, 1992) – (1832, 1852, 1862, 1888, 1899, 1919, 1937, 1957, 1977, 1990)] = [6, 7, 3, 6, 7, 6, 6, 6, 0, 2], a mean coincidence of 4.8 years. This mean at the 74-year NAO winter index has a maximum speed in negative direction, to less cold winds and more warm winds, when the Barents Sea temperature and the Barents Sea ice position have a maximum state.

Upcoming NAO index events

The stationary 74-year period in the NAO index variability have computed upcoming phase-shifts of: Wnao(s(74), Fnao) = [(+0, 2017), (min, 1957 + 74 = 2031), (-0, 1977 + 74 = 2051), (max, 1990 + 74 = 2064), (+0, 2017 +74 = 2091), (min, 2031 + 74 = 2105)]. The NAO index was turning in 2017. In Scandinavia, from a period associated with warm winds from west, mild winters and rain-full summers, to a period of cold winters and less rain-full summers. More cold winds for 2017 to a maximum at 2064 and more warm winds from 2091.

The Barents Sea ice edge wavelet power spectrum has identified amplitude- and phase-shifts at: WPie(s(223), Fie) = [(+0, 1580), (-97.0, 1644), (-0, 1680), (+80.5, 1726), (+0, 1781), (-69.0, 1845), (-0, 1910), (+56.0, 1979)] in periods of 223 years. A π/2 (rad) phase-lag from the 223-year ice edge position period to a 223-year NAO index period, is expected to have amplitude- and phase-shifts approximately at: Wnao(s(223), Fnao) = [(max, 1580), (+0, 1644), (min, 1680), (-0, 1726), (max, 1781), (+0, 1845), (min, 1910), (-0, 1979)]. Computed upcoming amplitude- and phase-shifts are: Wnao(s(223), Fnao) = [(-0, 1979), (max, 1781 + 223 = 2004), (+0, 1845 + 223 = 2068), (min, 1910 + 223 = 2133), (-0, 2202)]. The upcoming 223-year NAO-index period reveals a modern maximum at the year 2004 and a (+0) phase-shift in 2068 when the 74-year NAO index period has a minimum. The long period has a deep minimum at 2133, close to the 74-year computed deep minimum at 2105. The 223-year period has a next positive NAO index period from 2203.

4 Discussion

4.2 The Arctic ice position variability

The data series

The Barents Sea ice edge position data series cover a time period of 439 years from 1579 to 2018. In this time period we may estimate periods up to 220 years. From 1800 to 2018 the data series have 153 recorded samples and 66 spline interpolated samples. From 1579 to 1800 the data series have 83 recorded samples and 138 spline interpolated samples. This limited number of recorded samples introduces a serious noise spectrum that may ruin the period estimates. From 1579 to 2018 the data series is cubic spline interpolated and analyzed be computing the wavelet power spectrum. The spline interpolation has the ability to preserve the investigated period spectrum in the data series. At the same time the interpolations may compute some unexpected interpolated maxima and minima. At the same time, the spline interpolation has an ability to preserve the period spectrum.

To get the best estimates, the lunar period spectrum is estimated from 1800 to 2018, where there missing data are estimated by spline cubic (MATLAB) interpolation. In this time period the data series is confirmed by a close period- and phase-coincidence to the Barents Sea (Kola) temperature data series. The data series analysis from 1579 to 2018 is based on a wavelet power spectrum analysis. The wavelet power spectrum has the ability integrate the long trends in the data series. The identified long trend is the 223-period, which is supported by the close coincidence to identified 12*18.6 and 3*74.4 = 223 year lunar periods.

Main results

The investigation confirms a lunar-driven Barents Sea ice edge position variability. The variability has a coincidence to the deterministic lunar period spectrum of [8.8, 18.6, 2*18.6 = 37.2, 4*18.4 = 74.4, 3*4*18.6 = 223] (yr). The mean difference between the stationary lunar period spectrum and the identified period spectrum is only 1 year. The Barents Sea ice edge position variability is period- and phase-locked to the Barents Sea Kola-section temperature variability from 1900. The period phase-coincidence between Barents Sea variability and ice edge position variability has a mean difference of only 2 years (Ref. Note). This close relation confirm that the Barents Sea ice position has a major ocean temperature-driven variability, controlled by a lunar spectrum.

Other investigations

The results are confirmed by other investigations. Yndestad (2006) studied the area of the Barents Sea ice extent which covers the Norwegian Sea, the Barents Sea, and the Kara Sea bounded by 10(E, 80(N, and 70(E, respectively. The data are based on April values from 1864 to 1998 (Vinje, 2001). The investigation identified lunar periods of [18.6/2, 18.6, 4*18.7] (yr). The same found a relation to lunar periods in Arctic Ocean and lunar periods of [18.6/15, 18.6/3, 18.6, 4*18.6] (yr) in Polar position variability (Earth nutation). This indicate a possible resonance between North Atlantic Water inflow and Polar position variability. The new information from the data series analysis is the identification of the 223-year lunar period. The source of his period is most likely inflow of North Atlantic Water. The phase-coincidence between the 75-year period and the 223-year period explains the long period of increased BIE position from 1800 to 2000.

Explanation

The period- and phase-coincidence Barents Sea ice position and Barents Sea temperature confirm that ice edge position is controlled by the Barents Sea water temperature, which is controlled by inflow of warm North Atlantic Water. Warm Atlantic water inflow to the Barents moves the ice edge position to a higher degree position. Cold Atlantic water inflow moves the ice edge to a reduced degree position.

Arctic Ocean Deep Water

Deep Water residence time in the Eurasian Basin is estimated to be about 75 years (Bonisch and Schlosser, 1995). This 75- year residence time is the same cycle period identified in polar motion, and in the extent of ice in the Barents Sea and Greenland. In the Amundsen Basin, Bottom Water (depth

>2600m) residence time is estimated to be 290 □+/- 30 years (Bonisch and Schlosser, 1995). A 290-year residence time is a fourth sub-harmonic of the 75- year cycle in the upper Deep Water. Inflow to the Arctic Ocean passes from the North Atlantic through the Barents Sea and the eastern Fram Strait, with a minor inflow from the Bering Strait.

Implications

The Barents Sea ice edge position variability is controlled by periods- and phase-relation in the lunar spectrum. The Barents Sea ice edge position is increased from 76 (deg) to 81 (deg) in the time period 1800 to 2018. The increased position in the time period is controlled by the phase-relations between the long stationary periods of 74 and 223 years. The same long stationary periods have a maximum at 2009 and 1977, upcoming temporary minimum in 2053 and a next deep minimum period from 2081 to 2127 A.D. This mean that Barents Sea ice edge position is expected to be reduced from 81 (deg) level to a 76 (deg) level the next 60 years and stay approximately at this deep minimum from 2080 to 2130.

4.3 The Barents Sea temperature variability

The wavelet spectrum of Barents Sea Kola-section temperature variability from 1900 to 2016 is controlled by a deterministic lunar period spectrum [18.6/2, 18.6, 2*18.6 = 37.2, 4*18.4=74.4] (yr). The period coincidence to BIE has a difference of 1 year, the phase coincidence has a mean difference of 1.7 years.

Explanation

The oscillation gravity between the Earth, Sun and the Moon causes an 18.6-year wobbling of the Earth axis and a standing 18.6-year lunar nodal tide between Equator and the Pole (Maximov and Smirnov, 1964, 1966, 1967), (Royer, 1993), (Currie, 1984), (Keeling and Worf, 1997), (Hansen el. Al 2015). The lunar nodal tide has a vertical amplitude direction and a horizontal current direction that causes a circular mixing of temperature profiles in the Atlantic Ocean. The stationary 18.6-year circular mixing of non-linear temperature profiles in ocean currents, causes a modulation of a lunar period spectrum in the Atlantic Ocean surface temperature variability. The modulated lunar controlled temperatures spectrum in the Atlantic Ocean follows North Atlantic Water inflow to the Norwegian Sea and three years later as inflow to the Barents Sea (Maximov and Smirnov, 1964, 1965, 1967), (Yndestad, 1999, 2006) (Yndestad et. al 2008).

Implications

The implication a lunar spectrum in Barents Sea temperature variability is a lunar period influence on ice edge position, the Barents Sea eco system and Arctic climate. The lunar temperature variability of Atlantic inflow influences the Barents Sea eco system food chain. Currie and Wyatt (1995) identified 18.6-year periods in Barents Sea cod biomass variability. Yndestad, (1999, 2009) identified a [18.6/3, 18.6/2, 18.6, 3*18.6] (yr) lunar spectrum in the variability of Plankton, Capelin, Herring and North Atlantic Cod. The implication of a Barents Sea temperature reduction the next to a deep minimum from 2080 to 2130, is expected to have a dramatic influence on the biomass growth in the Barents Sea.

4.5 The NAO index variability

The NAO winter index variability from 1822 to 2017 is period- and phase-locked to the Barents Sea ice edge position variability, at a phase-lag of $\pi/2$ (rad). NAO winter index periods have a minimum when Barents Sea ice edge position period has a phase-shift to a positive state. The period coincidence to the lunar spectrum has a mean difference of only 1 year. The phase-coincidence between ice position periods and NAO periods have a difference of 6 years.

Explanation

The relation between ice position variability and NAO winter index variability may be explained by an ice position that represents an isolator between the warm sea surface and the cold Arctic air temperature. The ice edge position then has an influence on the Arctic wind direction and the NAO winter index. The 6 year phase-lag from Barents Sea ice edge position to the NAO index, may be explained by an influence from Greenland ice edge position (Yndestad, 2006).

Implications

The wavelet spectrum analysis reviles that long-term weather conditions Northern Europe are controlled by deterministic lunar periods up to 223 years in North Atlantic Water. The NAO periods have a $\pi/2$ (rad) phase-lag from ice edge position. The 74-year NAO period turned into a negative state from 2017 to a computed minimum in 2013. This confirm a maximum ice edge position close to the year 2017. The upcoming 223-year NAO-index period show a maximum at the year 2004, phase-shift in negative direction from 2068 when the 74-year NAO index period has a minimum. The long 223-year period has a deep minimum at 2133, close to the 74-year computed deep minimum at 2105 and a next 223-year positive NAO index period from 2203. The implication of a coincidence between the identified 74-year and the 223-year lunar period, is an upcoming long period of cold winds and deep cold climate in Scandinavia and North-Europe. This cold climate period has a computed minimum close the 2100 A.D. and a computed turning point at 2203 A.D.

REFERENCES

Currie, R. G., 1984, Evidence for 18.6-year (*sic*) lunar nodal (*sic*) drought in western North America during the past millennium: Journal of Geophysical Research. 89:1295-1308.

Currie, R. G., 1981, Evidence for 18.6 year (*sic*) signal in temperature and drought conditions in North America since A. D. 1800: Journal of Geophysical Research. 86:11,055-11,064.

Currie, R. G., 1984, Evidence for 18.6 year (*sic*) lunar nodal (*sic*) drought in western North America during the past millennium: Journal of Geophysical Research. 89:1295-1308.

Currie, R. G., 1987, Examples and implications of 18.6- and 11-yr terms in world weather records, Chap. 22, p. 378-403 *in* Rampino, M. R.; Sanders, J. E.; Newman, W. S.; and Konigsson, L.-K.; *eds*., Climate: History, periodicity, and predictability: International Symposium held at Barnard College, Columbia University, New York, New York, 21-23 May 1984 (R. W. Fairbridge Festschrift): New York, NY, Van Nostrand Reinhold Publishing Corp., 588 p.

Currie, R. W.; Wyatt, Tim; and O'Brien, D.P, 1993. Deterministic signals in European fish catches, wine harvests, sea level, and further experiments: International Journal of Climatology. 8:255-281.

DICKSON R R, T. J. OSBORN, J. W. HURRELL, J. MEINCKE, J. BLINDHEIM, B. ADLANDSVIK, T. VINJE, G. ALEKSEEV, AND W. MASLOWSKI (2000), The Arctic Ocean Response to the North Atlantic Oscillation. Journal of Climate. Vol. 13. 2671-2696.

Egbert, G.D., Ray, R.D., 2000. Significant dissipation of tidal energy in the deep ocean from ocean inferred from satellite alitimeter data. Nature 405 (6788), 775–778.

Hansen, J. M., Aagaard, T., & Kuijpers, A. (2015). Sea-Level Forcing by Synchronization of 56- and 74-Year Oscillations with the Moon's Nodal Tide on the Northwest European Shelf (Eastern North Sea to Central Baltic Sea). *Journal of Coastal Research*, *315*(1991), 1041–1056. http://doi.org/10.2112/JCOASTRES-D-14-00204.1

Keeling, Charles D. and T. P. Whorf. 1997. Possible forcing global temperature by oceanic tides. Proceedings, National Academy of Sciences of the United States. 94:8321-8328.

Lindquist, A. 2002. Herring periods of Bohuslan: a cross-sectorial approach. ICES Marine Science Symposia, 215: 343-351.

Ljungman, A. V. 1879. Bidrag till løsningen af frågan om de stora sillfiskenas sekulära periodisitet. Tidskrift for Fiskeri, 5: 257-268. (In Swedish).

Maksimov, I. V. and Smirnov, N. P. 1964. Long-range forecasting of secular changes of the general ice formation of the Barents Sea by the harmonic component method. Murmansk Polar Sci. Res. Inst., Sea Fisheries, 4: 75-87.

Maksimov, I. V. and Smirnov, N. P. 1965. A contribution to the study of causes of long-period variations in the activity of the Gulf Stream. Oceanology. 5:15-24.

Maksimov, I. V. and Smirnov, N. P. 1967. A long-term circumpolar tide and its significance for the circulation of ocean and atmosphere. Oceanology 7: 173-178 (English edition).

Maksimov, I. V. and Sleptsov-Shevlevich, B. A., 1970. Long-term changes in the tide-generation force of the moon and the iciness of the Arctic Seas. Proceedings of the N. M. Knipovich Polar Scientific-Research and Planning Institute of Marine Fisheries and Oceanography (PINRO). 27: 22-40.

Pettersson, O. 1905. On the probable occurrence in the Atlantic current of variations periodical, and otherwise, and their bearing on metrological and biological phenomena. Rapports et Proce`s-Verbaux des Re´unions de Conseil Permanent International pour l'Exploration de la Mer, 42: 221e240

Royer Thomas C. 1993. High-Latitude Oeanic Varibility Associated With the 18.6-Year Nodal Tide. Journal of Geophysical Research. 98: 4639-4644.

Smedsrud, L. H., et al. (2013), The role of the Barents Sea in the Arctic climate system, Rev. Geophys., 51, doi:10.1002/rog. 20017.

Yndestad, H: 1999. Earth nutation influence on the temperature regime of the Barents Sea. ICES Journal of Marine Science; 56; 381-387. 1999.

Yndestad, H. (2006). The influence of the lunar nodal cycle on Arctic climate. *ICES Journal of Marine Science*, *63*(3), 401–420. http://doi.org/10.1016/j.icesjms.2005.07.015

Yndestad H. 2004 The Lunar nodal cycle influence on the Barents Sea. Dr. philos. Thesis. NTNU. Trondheim, Norway.

Yndestad, H. (2007). The Arctic Ocean as a Coupled Oscillating System to the Forced 18.6 Year Lunar Gravity Cycle. In J. B. (Eds. Tsonis, Anastasios A., Elsner (Ed.), *Nonlinear Dynamics in Geosciences* (pp. 281–290). New York: Springer New York.

Yndestad, H., Turrell, W. R., & Ozhigin, V. (2008). Lunar nodal tide effects on variability of sea level, temperature, and salinity in the Faroe-Shetland Channel and the Barents Sea. *Deep-Sea Research Part I: Oceanographic Research Papers*, *55*(10), 1201–1217. http://doi.org/10.1016/j.dsr.2008.06.003.

Yndestad, H. (2009). The influence of long tides on ecosystem dynamics in the Barents Sea. *Deep-Sea Research Part II: Topical Studies in Oceanography*, *56*(21–22), 2108–2116. http://doi.org/10.1016/j.dsr2.2008.11.022